Translational Oncology 16 (2022) 101322

Contents lists available at ScienceDirect

Translational Oncology

journal homepage: www.elsevier.com/locate/tranon

Original Research

NHS-IL12 and bintrafusp alfa combination therapy enhances antitumor activity in preclinical cancer models

Chunxiao Xu *, Bo Marelli, Jin Qi, Guozhong Qin, Huakui Yu, Hong Wang, Molly H. Jenkins, Kin-Ming Lo, Yan Lan *

EMD Serono Research and Development Institute, Inc, 45 Middlesex Turnpike, Billerica, MA 01821, USA

ARTICLE INFO

Key words:
TGF-β
Anti–PD-L1
Immunocytokine
NHS-muIL12

ABSTRACT

Combinatorial immunotherapy approaches are emerging as viable cancer therapeutic strategies for improving patient responses and outcomes. This study investigated whether two such immunotherapies, with complementary mechanisms of action, could enhance antitumor activity in murine tumor models. The immunocytokine NHS-IL12, and surrogate NHS-muIL12, are designed to deliver IL-12 and muIL-12, respectively, to the tumor microenvironment (TME) to activate NK cells and $CD8^+$ T cells and increase their cytotoxic functions. Bintrafusp alfa (BA) is a bifunctional fusion protein composed of the extracellular domains of the TGF-β receptor II to function as a TGF-β "trap" fused to a human IgG1 antibody blocking PD-L1. With this dual-targeting strategy, BA enhances efficacy over that of monotherapies in preclinical studies. In this study, NHS-muIL12 and BA combination therapy enhanced antitumor activity, prolonged survival, and induced tumor-specific antitumor immunity. This combination therapy increased tumor-specific $CD8^+$ T cells and induced immune profiles, consistent with the activation of both adaptive and innate immune systems. In addition, BA reduced lung metastasis in the 4T1 model. Collectively, these findings could support clinical trials designed to investigate NHS-IL12 and BA combination therapy for patients with advanced solid tumors

Introduction

Cancer immunotherapies, such as immune checkpoint inhibitors (ICIs), have revolutionized cancer treatment in the past decade, resulting in clinical success for many patients with advanced cancer. However, response rates remain relatively low and, in certain cancers, immunotherapies have little or no effect on patient response or survival [1]. Emerging evidence suggests that the presence of intratumoral T cells plays a major role in patient sensitivity to ICIs [2], such as anti–programmed death (ligand) 1 PD-(L)1. Predictors of poor prognosis with these therapies include lack of tumor infiltrating lymphocyte (TIL) populations [3,4], low activity of type 1 T-helper (Th1) cells, reduced immune cytotoxicity in the TME [5], as well as increased immunosuppressive pathways, such as levels of transforming growth factor-β (TGF-β) [6,7]. Therefore, boosting innate and adaptive immunity by enhancing pro-inflammatory pathways, while also targeting tumor immunosuppressive pathways, offers a rational therapeutic strategy [1]. Synergistic combinations provide an opportunity to enhance the therapeutic benefit of immunotherapeutics by targeting different components of tumor progression and immune escape, and appear to be promising for future therapies [8]

Interleukin-12 (IL-12) is a pro-inflammatory cytokine, released by dendritic cells (DCs) and phagocytes during T cell priming [9], that stimulates proliferation and increases cytotoxicity of natural killer (NK), natural killer T (NKT) cells, and $CD8^+$ T cells [10]. IL-12 induces cytokines, such as interferon gamma (IFN-γ), which function to stimulate both innate and adaptive cytotoxic immune effector cells, leading to immune surveillance and antitumor immune responses [10–16]. Sustained IL-12 signaling can drive naive Th cell differentiation to the Th1 lineage via the activation of STAT4 [11,17]. Therapeutic administration of IL-12 is therefore a promising strategy to promote immunostimulatory antitumor effects and has been investigated by multiple clinical centers as a monotherapy or in combination with chemotherapy [18–21]. However, systemic side effects and narrow therapeutic windows limit the clinical application of IL-12 therapies. The NHS-IL12 immunocytokine, composed of the human monoclonal immunoglobulin G1 (IgG1) antibody NHS76 fused at each CH_3 C-terminus to IL-12, was designed to direct IL-12 to intratumoral necrotic regions, thereby

* Corresponding author.
E-mail addresses: chunxiao.xu@emdserono.com (C. Xu), yan.lan@emdserono.com (Y. Lan).

https://doi.org/10.1016/j.tranon.2021.101322
Received 10 November 2021; Received in revised form 6 December 2021; Accepted 17 December 2021
1936-5233/© 2021 Published by Elsevier Inc. This is an open access article under the CC BY-NC-ND license (http://creativecommons.org/licenses/by-nc-nd/4.0/).

alleviating safety concerns associated with systemic administration of recombinant IL-12 and improving its pharmacokinetics [22]. In a phase I clinical trial (NCT01417546), NHS-IL12 treatment was well-tolerated and enhanced immune-related activity, including evidence of increased immune infiltration in the TME of patients with metastatic solid tumors [23]. These results from early clinical trials suggest that NHS-IL12 can prime nonimmunogenic tumors and may further trigger the antitumor immune response to ICIs, indicating that further studies are warranted, particularly the combination of NHS-IL12 with ICIs

In murine tumor models, NHS-muIL12, the chimeric surrogate of NHS-IL12, stimulates proliferation and cytotoxic function of immune effector cells, including NK cells and $CD8^+$ T cells, induces the differentiation of naïve Th cells towards a Th1 phenotype, and increases the production of cytokines including IFN-γ [24]. NHS-muIL12 also elicits antitumor activity in preclinical mouse models as a monotherapy and in combination with an anti–PD-L1 IgG1 antibody [24]. The complementary immune stimulatory effects of NHS-muIL12 and anti–PD-L1 enhanced antitumor activity in combination therapy compared with either monotherapy in two preclinical tumor models [24]. Results from this study suggest that NHS-muIL12 alters the TME by enhancing immune cell infiltration and sensitizing tumors to the effects of anti–PD-L1 therapy. These results supported the development of a phase Ib trial with NHS-IL12 in combination with the anti–PD-L1 antibody avelumab (NCT02994953), which has reported an acceptable safety and tolerability profile, leading to a recommended phase II dose (RP2D) [25]

The combination of NHS-IL12 with therapies targeting other immunosuppressive pathways, such as TGF-β, provides another rational therapeutic strategy. TGF-β is a pleiotropic cytokine that can promote tumor progression and facilitate tumor immune evasion through its suppressive effects on the innate and adaptive immune systems, or within the TME, through its induction of stromal modifications, angiogenesis, and epithelial-mesenchymal transition (EMT) [26–28]. Several studies have shown that TGF-β can reduce the response of lymphocytes to IL-12 stimulation by inhibiting their IFN-γ production [29–31], and others have found that TGF-β can suppress IL-12-mediated immune modulation by interfering with the IL-12 signal transduction pathway [31,32]. During antigen priming and T cell activation, TGF-β can downregulate IL-12 receptor expression, blocking the JAK-STAT4 pathway and thereby inhibiting IL-12-mediated modulation of the immune response [29]. On activated T cells, TGF-β directly inhibits JAK2, TYK2, and STAT4 phosphorylation, inducing unresponsiveness to IL-12 [29].

Bintrafusp alfa (BA) is a bifunctional fusion protein composed of the extracellular domains of the human TGF-β receptor II (TGF-βRII or TGF-β trap) fused via a flexible linker to the C-terminus of each heavy chain of a human anti–PD-L1 IgG1 antibody, designed to simultaneously target both TGF-β and PD-L1 pathways [33]. In preclinical models, BA can enhance antitumor activity and prolong survival relative to anti–PD-L1 and TGF-β trap controls [33]. In preclinical models, BA was shown to activate both the innate and adaptive immune systems and provide long-term protective antitumor immunity, reduce metastasis and fibrosis, and be an effective combination partner with radiation or chemotherapy [33,34]. In phase I clinical trials in patients with advanced solid tumors, BA showed early evidence of clinical activity [35–40].

Here we report that NHS-muIL12 and BA combination therapy enhanced antitumor efficacy and extended survival compared with either monotherapy in syngeneic mouse tumor models. NHS-muIL12 and BA combination therapy also induced the generation of tumor-specific immune memory, as demonstrated by protection against tumor rechallenge, and stimulated proliferation and priming of immune effector cells. In addition, combination therapy decreased spontaneous metastasis, which was driven mainly by BA. These preclinical findings could support potential clinical development of NHS-IL12 and BA combination therapy or triple combination with NHS-IL12, BA, and chemo-radiation therapy [41,42] for the treatment of patients with advanced solid tumors.

Materials and methods

Mice

All animal procedures were performed in accordance with institutional protocols approved by the Institutional Animal Care and Use Committee (IACUC) of EMD Serono Research and Development Institute; animal care was in accordance with institutional guidelines. BALB/c Igh-J^{tm1Dhu} (Jh) B cell deficient mice were purchased from Taconic, B6.129S2-^{Ighmtm1Cgn}/J C57BL/6 (μMt^-) were purchased from The Jackson Laboratory, and BALB/c and C57BL/6 mice were purchased from Charles River Laboratories. All mice used for experiments were 8 to 12-week-old females. Mice were housed with ad libitum access to food and water in a pathogen-free facility.

Cell lines

EMT-6 and 4T1 breast cancer cell lines were obtained from the American Type Culture Collection (ATCC, Manassas, VA). The MC38 colon carcinoma cell line was provided by the Scripps Research Institute (La Jolla, CA). All cell lines were tested and verified to be free of *Mycoplasma*. EMT-6 cells were maintained in Waymouth's medium (Gibco) and 15% heat-inactivated fetal bovine serum [FBS] (Life Technologies). 4T1 cells were cultured in RPMI 1640 supplemented with 10% FBS and MC38 cells were cultured in Dulbecco's Modified Eagle Medium (DMEM) supplemented with 10% FBS. All cells were cultured under aseptic conditions and incubated at 37 °C with 5% CO_2. Cells were passaged at least twice prior to *in vivo* implantation and harvested with TrypLE Express (Gibco) or 0.25% trypsin. Prior to experiments, trypan blue exclusion staining was used to determine the number of viable cells.

Murine tumor models

Subcutaneous MC38 tumor model

μMt^- mice were inoculated subcutaneously (sc) into the right flank with 0.5×10^6 MC38 cells and tumor growth and survival were measured. For efficacy experiments, treatment was administered when the average tumor volume reached 50–100 mm^3. For flow cytometry and enzyme-linked immunospot (ELISpot) studies, treatment was administered when the average tumor volume reached 300–400 mm^3, and mice were sacrifice on Day 6 post treatment start.

For MC38 tumor rechallenge studies, C57BL/6 mice with complete remission of MC38 intramuscular (im) tumors for over 3 months after the last treatment of BA (164 μg, intravenously [iv], Days 0, 2, 4) monotherapy ($n = 2$ mice) or BA + NHS-muIL12 (5 or 25 μg, sc, Day 0) combination therapy ($n = 6$ mice) were injected sc with 0.1×10^6 MC38 tumor cells into the opposite flank from the original tumor site. As a control, naïve C57BL/6 mice ($n = 10$ mice) were injected sc with tumor cells in the flank.

Orthotopic EMT-6 tumor model

To generate the EMT-6 tumor model, BALB/c mice were inoculated with 0.5×10^6 EMT-6 tumor cells orthotopically in the mammary fat pad.

For EMT-6 cured tumor rechallenge studies, mice with complete remission of EMT-6 tumors for over 3 months after the last treatment of NHS-muIL12 (5 or 10 μg, sc, Day 0) ($n = 7$ mice), BA (492 μg, iv, Day 0, Day 7, or Days 0, 3) ($n = 4$ mice), or BA + NHS-muIL12 combination therapy ($n = 26$ mice) were injected with 0.25×10^6 EMT-6 tumor cells or 0.5×10^5 4T1 tumor cells into the opposite mammary pad from the original tumor site. As a control, naïve BALB/c mice were injected with EMT-6 cells ($n = 10$ mice) or 4T1 cells ($n = 10$ mice) in the mammary pad.

Orthotopic 4T1 tumor model

To generate the 4T1 tumor model, Jh mice were inoculated with 0.5 × 10^5 4T1 tumor cells orthotopically in the mammary fat pad.

Treatments

For all studies, mice were randomized into treatment groups on the day of treatment initiation. The inactive anti–PD-L1 control (hereafter referred to as isotype control) is a mutated anti–PD-L1 antibody without the ability to bind PD-L1. Isotype control, BA, and NHS-muIL12 were produced and purified at EMD Serono.

NHS-muIL12

In tumor-bearing mice, NHS-muIL12 (2, 10, or 25 μg) was administered sc in 0.1–0.2 mL PBS. Exact doses for each experiment are listed in the figure legends; all tumor-bearing mice were treated with a single dose of NHS-muIL12 at Day 0.

BA and controls

In tumor-bearing mice, BA (492 μg) or isotype control (anti–PD-L1 [*mut*], 400 μg) were administered iv in 0.1–0.2 mL PBS as previously described [33]. Exact doses and treatment schedules for each experiment are listed in the figure legends. Briefly, B cell–deficient Jh or μMt–tumor-bearing mice were treated twice per week for three continuous weeks. Because BA is a recombinant human protein and induces a strong immunogenic response in immunocompetent mice if dosed repeatedly for more than 6 days [33], B cell–deficient mouse strains (Jh and μMt–) were used *in vivo* studies to enable testing of clinically-relevant repeat dosing schedules, unless otherwise indicated. Wild-type tumor-bearing mice were treated at Days 0, 2, and 4.

Tumor growth and survival

Tumor size was measured twice weekly with digital calipers and recorded automatically to a computer using WinWedge software. Tumor volumes were calculated using the following formula: tumor volume (mm^3) = tumor length × width × height × 0.5236. Tumor growth inhibition (TGI) was calculated using the following formula: TGI (%) = [1 – (Ti-T0)/(Vi-V0)] x 100, where Ti is the average tumor volume (mm^3) of a treatment group on a given day, T0 is the average tumor volume of the treatment group on the first day of treatment, Vi is the average tumor volume of the vehicle control group on the same day as Ti, and V0 is the average tumor volume of the vehicle control group on the first day of treatment. For the MC38 model, body weight was measured twice weekly, and mice were euthanized if their tumor volume exceeded 2500 mm^3. For the EMT-6 and 4T1 orthotopic models, mice were euthanized when their tumor volume reached 1000 mm3. Kaplan-Meier survival curves were generated to compare the percentage survival between treatment groups.

Rechallenge studies

For tumor rechallenge studies, mice from 2 to 3 separate studies that showed complete regression of MC38 or EMT-6 tumors for over 3 months after the last treatment of NHS-muIL12 and BA combination therapy or BA monothreapy were injected with MC38 or EMT-6 tumor cells into the opposite side of the original tumor location. As a control, naïve C57BL/6 (for MC38) and BALB/c (for EMT-6) mice were also injected with tumor cells

Metastasis

To assess metastases in the 4T1 model, mice were sacrificed on Day 25 and lungs were removed and placed in Bouin's fixation solution for subsequent scoring of lung nodules. Mice that were sacrificed prior to the end of study (Day 25) due to health concerns were not included as part of the metastasis analysis. However, mice that were sacrificed prior to Day 25 because they reached maximum tumor volume (1000 mm^3) were included in the analysis.

ELISpot assay

A mouse IFN-γ ELISpot assay was performed as previously described [24,33] to evaluate the frequency of IFN-γ producing $CD8^+$ T cells reactive to the tumor antigen p15E, a T cell rejection epitope expressed by MC38 tumors. On Day 6, spleens from mice in each treatment group (n = 6 mice/group) were harvested, pooled, and processed into single cell suspensions. $CD8^+$ T cells were isolated using a $CD8^+$ T cell isolation kit (Miltenyi Biotech) and the AutoMACS Pro-Separator. Antigen presenting cells (APCs) derived from splenocytes from naïve C57BL/6 mice were pulsed with the p15E epitope KPSWFTTL (20 μg/mL) (CPC Scientific) or the negative control ovalbumin (OVA) peptide SIINFEKL (20 μg/mL; CPC Scientific) for 1 h and then irradiated with 2000 rads in the GammaCell 40 Exactor. The peptide-pulsed, irradiated APCs (5 x 10^5 per well) were co-cultured with the isolated $CD8^+$ T cells (5 x 10^6 per well) in ELISpot assay plates (BD Biosciences) coated with purified anti-mouse IFN-γ antibody (BD Biosciences, Cat #51–2525KC). After incubation at 37 °C for 16 to 20 h, the cells were removed from the assay plate and IFN-γ was detected with a biotinylated anti-IFN-γ antibody (BD Biosciences, Cat #51–1818KZ) and a streptavidin-HRP detection conjugate (BD Biosciences, Cat #51–9,000,209) followed by a chromogenic substrate solution (3-Amino-9-Etylcarbazole, Sigma Cat #A6926). The number of IFN-γ–positive spots in each well of the assay plate was determined using an Immunospot ELISpot reader system (CTL-Immunospot S5UV Analyzer; Cellular Technology Limited). The data are presented as the mean ± SD of the number of spots/well (3 wells) and well images are displayed.

Tumor dissociation

For immunophenotyping studies, flow cytometry staining was performed on dissociated tumors and spleens using standard procedures as previously described . Mice were sacrificed at study Day 6 and tumors and spleens were harvested. Briefly, for preparation of tumor cell suspensions, tumors were harvested and finely minced with sterile scissors. Tumor cell suspensions for immunophenotyping stratification studies were additionally incubated in a solution of type IV collagenase (400 units/mL) and DNase 1 (100 μg/mL) for ~0.5 to 1 h at 37 °C with frequent agitation. Following tumor digestion, debris was separated by sedimentation, and suspensions were passed through a 70-μm nylon cell strainer. Cells were resuspended in DMEM containing 10% FBS. Single cell suspensions of splenocytes were obtained by mechanical disruption of tissue in 2% FBS-PBS and incubation with red blood cell lysis buffer (Sigma) followed by filtration through a 40-μm nylon cell strainer. For both tumor and spleen cell analyses, trypan blue was used to distinguish viable cells prior to staining, and 1 × 10^6 cells were used for flow cytometry analysis.

Flow cytometry

Antibody staining of tumor cell and splenocyte suspensions for flow cytometry analysis was performed following the antibody manufacturer's recommendations. Fluorophore-conjugated antibodies to NK1.1 (PK136), CD8a (53–6.7), CD4 (RM4–5), CD183 (CXCR3–173), CD25 (PC61), CD45 (30-F11), CD44 (IM7), CD69 (H1.2F3), and FoxP3 (FJk-16 s) were purchased from Biolegend, and the antibody to Ki-67 (MOPC-21) was purchased from BD Pharmingen. Viability Dye eFluor 455 (UV) and antibodies to CD62L (L-selectin) (MEL-14), T-bet (4B10), and EOMES (Dan11mag) were purchased from eBiosciences.

Cells were blocked with anti-CD16/CD32 (FcγRIII/FcγRII, 2.4G2) at a 1:25 dilution for 20 min, incubated with surface marker antibodies for 30 min on ice, stained with fixable viability dye for 30 min at 4 °C, and then permeabilized with BD Cytofix/Cytoperm buffer before intracellular labeling antibodies (Foxp3, T-bet, and Ki-67) were added for an overnight incubation at 4 °C. Cells were analyzed on a BD LSR II flow cytometer according to the manufacturer's instructions. Flow cytometry

analysis was performed using BD FACSDiva® software (V8). Cellular events were first gated by forward and side scatter characteristics and then by viability (Supplementary Fig. S1). Tumor and splenic cells were gated on immune cell subpopulations as described in the figure legends.

Statistical analysis

Statistical analyses were performed using GraphPad Prism Software, version 8.0.1; differences were determined to be significant if $p < 0.05$. To assess differences in tumor volumes between treatment groups, two-way analysis of variance (ANOVA) was performed followed by Tukey's multiple comparison test. Tumor volume data are presented graphically as mean ± standard error of the mean (SEM) or as individual tumor volumes, where each line represents data from individual mice. A Kaplan-Meier plot was generated to show survival by treatment group and significance was assessed by log-rank (Mantel-Cox) test. For flow cytometry analysis, data are displayed for individual mice (symbols) and means (horizontal line) and one-way ANOVA with Sidak's multiple comparison tests were used to compare treatment groups. For ELISpot analyses, bar graphs show mean and standard deviation (SD) and two-way ANOVA with Tukey's multiple comparison tests were used to compare treatment groups. To evaluate the difference in the number of lung modules between treatment groups, two-tailed unpaired t-tests were performed.

Results

NHS-muIL12 and BA combination therapy induces tumor regression in the MC38 model

To investigate the efficacy of NHS-muIL12 and BA combination therapy in a colorectal carcinoma model, mice bearing sc MC38 tumors were treated with NHS-muIL12 and BA. Significant TGI was induced by both NHS-muIL12 (TGI = 46.3%; $p < 0.0001$; Day 21) and BA (TGI = 47.2%; $p < 0.0001$; Day 21) monotherapies relative to isotype control (Fig. 1A and B). However, NHS-IL12 and BA combination therapy further enhanced TGI (94.9%; Day 21) relative to NHS-muIL12 ($p < 0.0001$) or BA ($p < 0.0001$) monotherapy (Fig. 1A and B**)**. The combination therapy also prolonged survival in MC38 tumor-bearing mice ($p = 0.0003$) (Fig. 1C). Complete tumor regression was observed in 2 of 8 (25%) mice treated with combination therapy (median survival = 45 days), compared with 0 of 8 (0%) mice treated with isotype control or NHS-muIL12 (median survival = 22 and 28 days, respectively) and 1 of 8 (12.5%) mice treated with BA monotherapy (median survival = 29.5 days) (Fig. 1C).

NHS-muIL12 and BA combination therapy induces protective antitumor immunity to tumor rechallenge in the MC38 tumor model

To assess whether mice with complete tumor regressions had established tumor-specific immune memory, a series of tumor rechallenge experiments were performed. Mice that had complete MC38 tumor regression for more than 3 months following BA monotherapy or

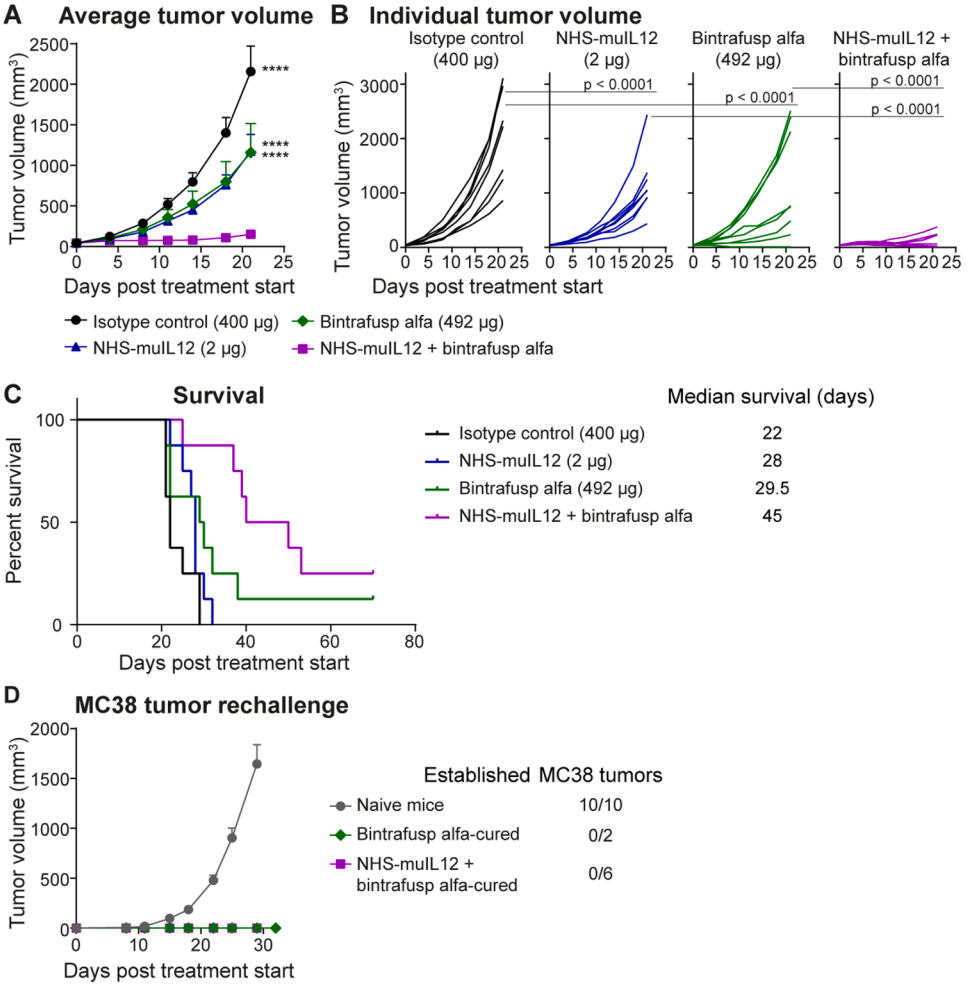

Fig. 1. NHS-muIL12 and BA combination treatment enhanced antitumor activity and induced long-term protective immunity in MC38 tumor-bearing mice. (A, B) Effect of NHS-muIL12 and BA on tumor growth. µMt$^-$ mice ($n = 8$ mice per treatment) were inoculated sc with 0.5 x 10^6 MC38 cells (Day −7) and treated with isotype control (400 µg iv; Days 0, 4, 7, 11, 14, 18, 21), NHS-muIL12 (2 µg sc; Day 0), BA (492 µg iv; Days 0, 4, 7, 11, 14, 18, 21), or NHS-muIL12 + BA. Tumor volumes (mm^3) were measured twice weekly and are presented as (**A**) mean ± SEM, where ****$p < 0.0001$ denotes a significant difference relative to combination therapy, or (B) individual tumor volumes, where each line represents an individual mouse. P-values were calculated by two-way ANOVA followed by Tukey's posttest. (C) A Kaplan-Meier survival curve and median survival times are shown. (D) Mice in complete remission for more than 3 months following last monotherapy ($n = 2$) or combination treatment ($n = 6$) and naïve C57BL/6 ($n = 10$) mice were challenged with 0.1 x 10^6 MC38 cells by sc injection on the opposite flank of the original tumor site. Average tumor volume after implantation is displayed with error bars representing SEM.

NHS-muIL12 and BA combination therapy were termed 'cured' mice. When these cured mice were rechallenged with MC38 cells (sc in the opposite flank from the original tumor), no tumor growth was observed in therapy-cured mice (0/6 mice), whereas treatment-naïve mice inoculated with MC38 cells rapidly developed tumors (10/10 mice, Day 29) (Fig. 1D), suggesting that the combination therapy generated tumor antigen specific long-term immune protective memory.

NHS-muIL12 and BA combination therapy elicits a distinct immune phenotype in MC38 tumor-bearing mice

To examine the potential mechanism by which NHS-muIL12 and BA combination therapy enhanced antitumor activity relative to monotherapies, immune cell populations within the TME and spleen were evaluated via flow cytometry analysis (see Supplementary Fig. S1 for gating strategy). In MC38 tumor-bearing μMt$^-$ mice, NHS-muIL12 and BA combination therapy significantly increased infiltrating CD8$^+$ T cells into the TME relative to isotype control ($p = 0.0011$) and NHS-muIL12 monotherapy ($p = 0.0049$), and trended towards increasing CD8$^+$ T cells relative to BA monotherapy (Fig. 2A). NHS-muIL12 and BA combination therapy significantly decreased the percentage of regulatory T cells (T_{regs}) in the TME relative to isotype control ($p = 0.0010$) and BA ($p = 0.0312$), but not relative to NHS-muIL12 monotherapy ($p > 0.05$). However, the ratio of CD8$^+$ TILs to infiltrating T_{regs} was significantly increased with combination therapy relative to both NHS-muIL12 ($p < 0.0001$) or BA ($p < 0.0001$) monotherapies (Fig. 2A), suggesting that BA and NHS-muIL12 combination therapy can convert an immune suppressive TME to a more immune activated phenotype.

The percentage of proliferating CD8$^+$ T cells in the tumor and spleen increased with combination therapy relative to NHS-muIL12 monotherapy ($p = 0.0051$ and $p < 0.0001$, respectively), though not relative to BA monotherapy ($p > 0.05$), suggesting that BA is the main driver responsible for CD8$^+$ T cell proliferation in the combination therapy (Fig. 2B). The percentage of CD8$^+$T cells expressing T-bet, a transcription factor important for T cell maturation, differentiation, and cytotoxicity, also increased in the tumors of mice treated with the combination therapy relative to those treated with NHS-muIL12 monotherapy ($p = 0.0002$) and increased in the spleen relative to NHS-muIL12 ($p < 0.0001$) or BA ($p < 0.0001$) monotherapy (Fig. 2B). The percentage of CD8$^+$ T cells expressing CXCR3, a chemokine receptor that regulates migration of cytotoxic T lymphocytes (CTLs), increased in both the tumor and spleen with combination therapy relative to NHS-muIL12 monotherapy ($p = 0.0019$ and $p = 0.0005$, respectively) and BA monotherapy ($p = 0.0481$ and $p = 0.0031$, respectively) (Fig. 2B), suggesting a potential additive effect from the single agents.

In addition to its effects on CD8$^+$ T cells, NHS-muIL12 and BA combination therapy also significantly increased the percentage of proliferating CD4$^+$ T cells in the spleen compared with either monotherapy (NHS-muIL12: $p < 0.0001$; BA: $p < 0.0001$) and trended towards increasing proliferating CD4$^+$ T cells in the TME compared with isotype control or NHS-muIL12 monotherapy (Fig. 2C). Combination therapy increased the percentage of T-bet$^+$ CD4$^+$ T cells in the tumor and spleen relative to NHS-muIL12 ($p < 0.0001$ and $p < 0.0001$, respectively) or BA ($p = 0.0151$ and $p < 0.0001$) monotherapy and increased the percentage of CXCR3$^+$ CD4$^+$ T cells in the tumor and spleen relative to NHS-muIL12 monotherapy ($p < 0.0001$ and $p < 0.0001$, respectively) and in the spleen relative to BA ($p < 0.0001$) monotherapy (Fig. 2C). Taken together, these data suggest that BA monotherapy has a more pronounced effect on CD8$^+$ and CD4$^+$ T cells in the tumor, and that adding NHS-muIL12 to BA can significantly increase CD8$^+$ and CD4$^+$ T cell immune response in both the periphery and TME.

Given that we observed induced antitumor immune memory with NHS-muIL12 and BA combination therapy in the rechallenge studies, we next investigated the presence of effector memory cells in the TME. We found that combination therapy significantly increased the percentage of CD8$^+$ effector memory T cells (T_{EM}) in the tumor relative to NHS-muIL12 monotherapy ($p < 0.0001$) and in the spleen relative to NHS-muIL12 ($p < 0.0001$) or BA ($p < 0.0001$) monotherapy (Fig. 2D)

Expression of NK1.1, a marker of NK cells in the MC38 model, was evaluated to determine the effect of treatment on the innate immune response. Although the activation (CD69$^+$) of NK cells was not significantly affected by BA monotherapy or combination therapy in the tumor ($p > 0.05$), NHS-muIL12 monotherapy trended towards increasing the percentage of CD69$^+$ NK cells in the tumor ($p = 0.0510$) and significantly increased these cells in the spleen ($p < 0.0001$) relative to isotype control. In the spleen, NHS-muIL12 and BA combination therapy further enhanced CD69$^+$ NK cells relative to NHS-muIL12 ($p < 0.0001$) or BA ($p < 0.0001$) monotherapy (Fig. 2E). In addition, combination therapy increased the percentage of NK cells in the spleen expressing the maturation marker EOMES, relative to NHS-muIL12 ($p = 0.0411$) or BA ($p < 0.0001$) monotherapy and showed trends towards increased cytotoxicity of infiltrated NK cell with T-bet expression (Fig. 2E). These data indicate possible synergy between the two molecules in the activation of an innate immune response, but suggest that NHS-muIL12 has a stronger effect than BA on NK cell activation.

To evaluate tumor antigen-specific T cell activation, the response of splenic CD8$^+$ T cells to p15E, an endogenous retroviral antigen expressed in MC38 tumor cells, was analyzed via ELISpot analysis. Relative to isotype control, the frequency of p15E-reactive, IFN-γ-producing CD8$^+$ T cells increased with monotherapy treatment of NHS-muIL12 (4.9-fold; $p = 0.0175$) or BA (5.6-fold; $p = 0.0052$). Combination therapy of BA and NHS-muIL12 further increased the frequency of p15E-reactive, IFN-γ-producing CD8$^+$ T cells compared with isotype control (25-fold; $p < 0.0001$), NHS-muIL12 (5.1-fold; $p < 0.0001$), or BA (4.4-fold; $p < 0.0001$) monotherapies (Fig. 3A and B)

NHS-muIL12 and BA combination therapy induces tumor regression and tumor-specific protective immunity in the EMT-6 model

The antitumor efficacy of NHS-muIL12 and BA combination therapy was next investigated in the EMT-6 syngeneic breast cancer model. In this model, significant TGI was induced by both NHS-muIL12 (TGI = 97.3%; $p < 0.0001$; Day 16) and BA (TGI = 41.4%; $p < 0.0001$; Day 16) monotherapies compared with isotype control treatment (Fig. 4A and B). However, NHS-muIL12 and BA combination therapy further enhanced TGI (TGI = 113.9%; Day 16) compared with NHS-muIL12 ($p < 0.0001$) and BA ($p < 0.0001$) monotherapies (Fig. 4A and B). The combination therapy also prolonged survival in EMT-6 tumor-bearing mice ($p < 0.0001$) (Fig. 4C). Complete tumor regression was observed in 9/10 (90%) of mice treated with the combination therapy (median survival > 100 Days), compared with 0/8 (0%) of mice treated with isotype control (median survival = 17 days), 1/10 (10%) of mice treated with BA (median survival = 19.5 days), or 5/10 (50%) of mice treated with NHS-muIL12 (median survival = 68.5 days) (Fig. 4C).

Mice that had complete EMT-6 tumor regression for more than 3 months following BA monotherapy, NHS-muIL12 monotherapy, or NHS-muIL12 + BA combination therapy were termed 'cured' mice. When these mice were rechallenged with EMT-6 cells, no tumor growth was observed in NHS-muIL12-cured (0/4 mice), BA-cured (0/4), or NHS-muIL12 and BA combination therapy-cured (0/16 mice). In contrast, treatment-naïve mice inoculated with EMT-6 cells (orthotopically) rapidly developed tumors (10/10 mice, Day 23) (Fig. 4D). When NHS-muIL12 or NHS-muIL12 + BA combination treatment-cured mice were challenged with 4T1 mammary tumor cells, all previously cured mice developed tumors (3/3 and 10/10 mice, respectively) at the same rate as naïve mice (10/10 mice) challenged with 4T1 cells ($p > 0.05$, Day 23) (Fig. 4E). Taken together, these data indicate that the NHS-muIL12 and BA combination therapy, as well as monotherapies, induced the generation of tumor antigen-specific immune memory.

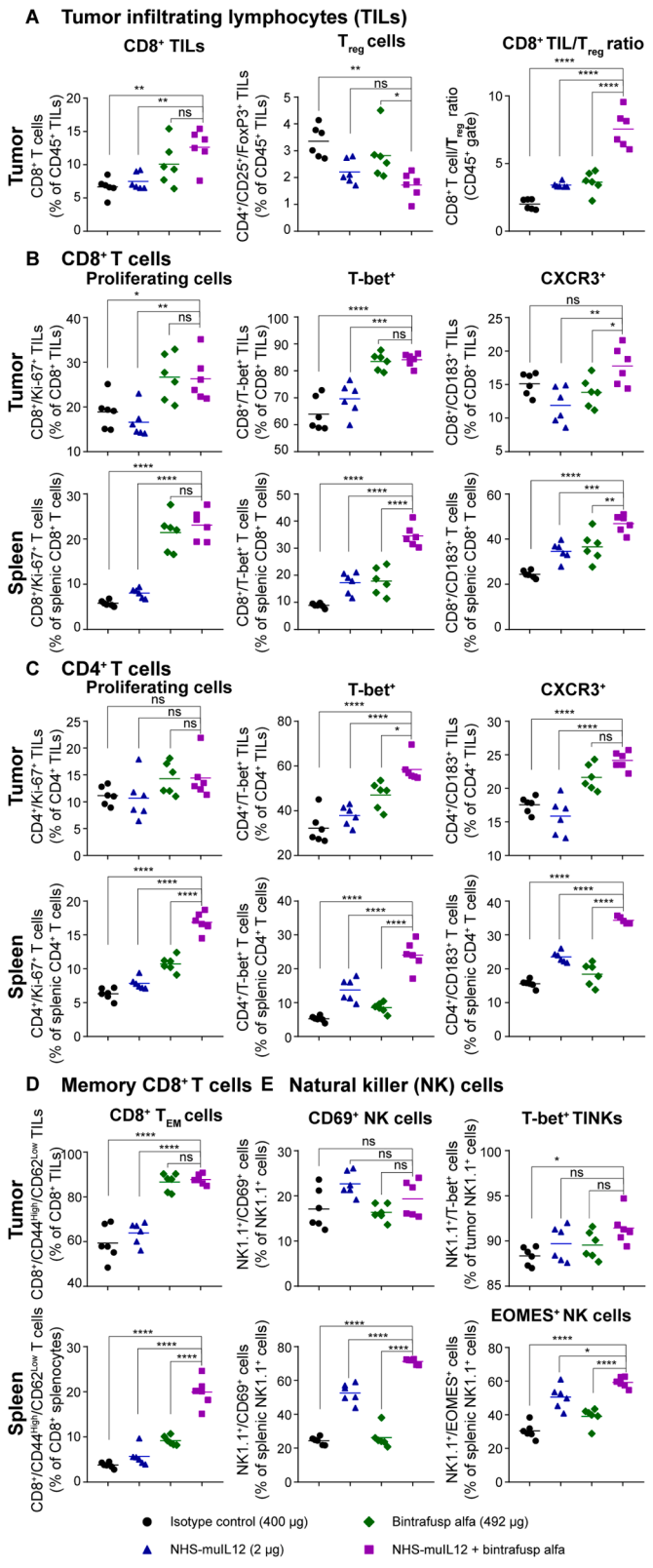

(caption on next column)

Fig. 2. NHS-muIL12 and BA combination therapy induced a distinct tumor immunophenotype in MC38 tumor-bearing mice. MC38 tumor-bearing μMt$^-$ mice ($n = 6$ mice per treatment) were treated with: isotype control (400 μg iv; Days 0, 2, 4), NHS-muIL12 (2 μg sc; Day 0), BA (492 μg iv Days 0, 2, 4), or NHS-muIL12 + BA. Flow cytometry analysis of dissociated tumors ($n = 6$ mice per group) harvested on Day 6 after treatment initiation was performed and percentages of populations were calculated. (A) TILs, including CD8$^+$ TILs and CD4$^+$CD25$^+$FoxP3$^+$ TILs (T_{regs}) in the CD45$^+$ gate and the ratio of CD8$^+$ TILs/T_{regs}. (B) CD8$^+$ T cells or (C) CD4$^+$ T cells in the tumor or spleen expressing markers for proliferation (Ki-67$^+$), T-bet$^+$, or CXCR3$^+$ (CD183$^+$). (D) Effector memory CD8$^+$ T cells (T_{EM}; CD44^{high}/CD62^{low}) in the tumor or spleen. (E) NK cells (NK1.1$^+$) expressing a marker of activation (CD69$^+$) in the tumor or spleen, T-bet$^+$ in the tumor, or EOMES$^+$ in the spleen. P-values were determined using one-way ANOVA followed by Sidak's posttest, where $^{****}p < 0.0001$, $^{***}p < 0.001$, $^{**}p < 0.01$, and $^{*}p < 0.05$ denote a significant difference relative to combination therapy; ns = not significant. In the plots, symbols represent individual mice and lines are the mean.

NHS-muIL12 and BA combination therapy and BA monotherapy suppresses spontaneous metastasis in the orthotopic 4T1 model

We next examined whether NHS-muIL12 and BA combination therapy or monotherapies could ameliorate spontaneous lung metastases in the 4T1 triple negative breast cancer model. Primary 4T1 orthotopic tumors were generated and metastatic nodules on the lung surface were evaluated at Day 25 post treatment start or when mice were sacrified because their tumors reached 1000 mm^3. Although NHS-muIL12 monotherapy had no significant effect on the number of lung tumor nodules ($p > 0.05$), BA monotherapy significantly reduced lung metastases ($p = 0.0183$) relative to isotype control (Fig. 5). NHS-muIL12 and BA combination therapy also reduced lung metastases relative to isotype control ($p = 0.0177$) and NHS-muIL12 monotherapy ($p = 0.0420$), although not relative to BA monotherapy ($p > 0.05$), suggesting that BA was likely the primary mediator of the reduction in lung metastases observed after combination therapy.

Discussion

We have previously shown that the immunocytokine NHS-IL12 alters the TME by enhancing immune cell infiltration and sensitizing tumors to the effects of anti–PD-L1 therapy [24]. In addition, we demonstrated that simultaneously blocking the PD-L1 and TGF-β pathways via the bifunctional fusion protein BA contributes synergistically to the molecule's antitumor efficacy, through activation of both the innate and adaptive immune systems [33]. Given the complementary mechanisms of action of NHS-IL12 and BA, combination of the two therapies is a rational strategy for the treatment of patients with solid tumors. In this study, we found that NHS-muIL12 and BA combination therapy enhanced antitumor activity in a colorectal carcinoma model in C57BL/6 mice as well as in a breast cancer model in BALB/c mice.

The enhanced antitumor effect with NHS-muIL12 and BA combination therapy may be mediated by both redundant and non-redundant mechanisms of the IL-12, PD-L1, and TGF-β pathways. Both NHS-muIL12 and BA have been shown to promote innate and adaptive immune responses and associated gene expression [24,33]. IL-12 plays an important role in regulating the transition from innate to adaptive immunity and acts directly on cytotoxic immune effector cells such as CD8$^+$ T cells and NK cells to stimulate proliferation and increase their cytotoxicity [10,14]. CD8$^+$ T cells and NK cells also play major roles in the antitumor activity of BA in the MC38 model [33]. We found that, in NHS-muIL12 and BA combination therapy, BA was the main driver promoting CD8$^+$ T cell proliferation, infiltration, and cytotoxicity, while

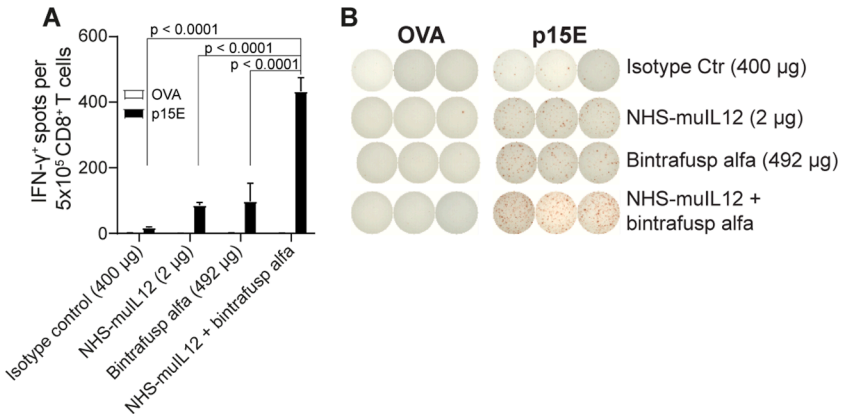

Fig. 3. Combination therapy with NHS-muIL12 and BA increased the frequency of p15E-specific IFN-γ-producing T cells. MC38 tumor-bearing μMt$^-$ mice ($n = 6$ mice/group) were treated with: isotype control (400 μg iv; Days 0, 2, 4), NHS-muIL12 (2 μg sc; Day 0), BA (492 μg iv Days 0, 2, 4), or NHS-muIL12 + BA. Splenic CD8$^+$ T cells from these MC38 tumor-bearing mice were incubated with APCs pulsed with OVA or p15E in an ELISpot assay. (A) The average number of IFN-γ$^+$ spots per 5×10^5 CD8$^+$ T cells were measured and (B) images of individual wells illustrate the IFN-γ production by CD8$^+$ T cells ("spots"). P-values were calculated using two-way ANOVA followed by Tukey's posttest. Error bars represent SD.

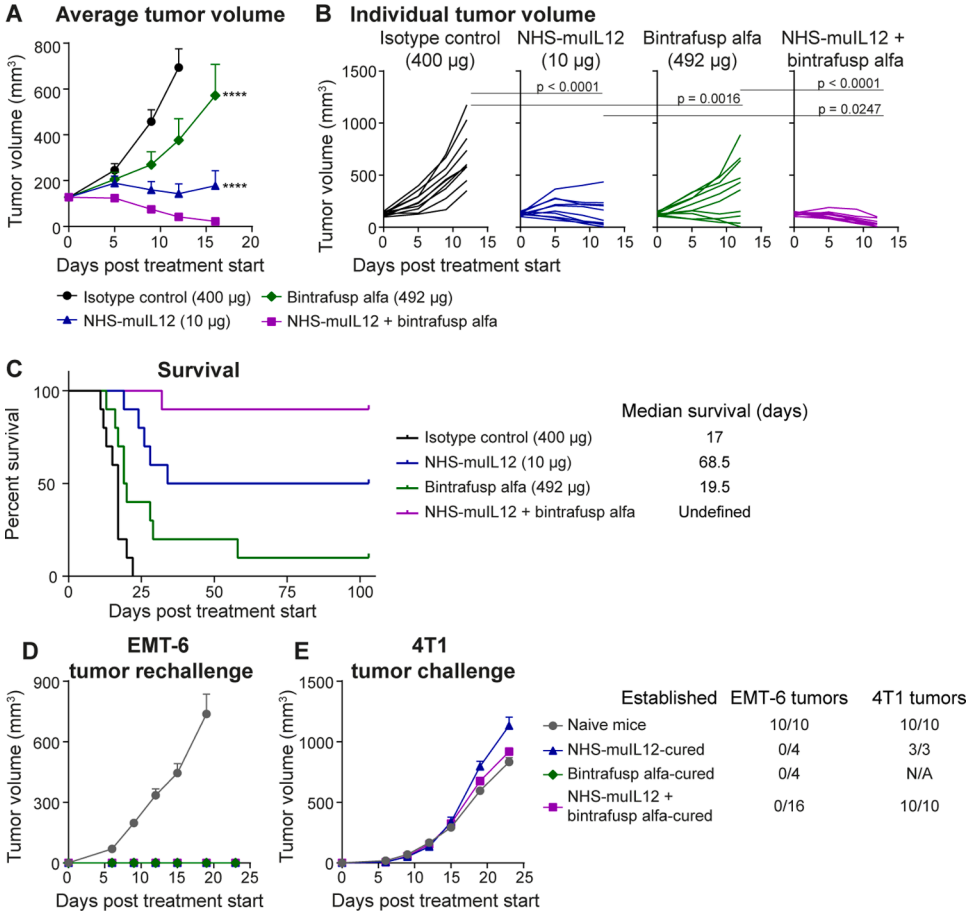

Fig. 4. Combination therapy with NHS-muIL12 and BA had a synergistic antitumor effect and induced long-term protective immunity in EMT-6 tumor-bearing mice. (A–C) EMT-6 tumor-bearing BALB/c mice ($n = 10$ mice/group) (~125 mm^3) were treated with: isotype control (400 μg iv; Day 0), NHS-muIL12 (10 μg sc; Day 0), BA (492 μg iv Day 0), or NHS-muIL12 + BA. (A) Average tumor volumes were measured twice weekly. Error bars represent SEM. P-values were calculated by log-transformation of tumor volume data and two-way ANOVA followed by Tukey's posttest, where $^{****}p < 0.0001$, $^{***}p < 0.001$, $^{**}p < 0.01$, and $^{*}p < 0.05$ denote a significant difference relative to combination therapy on Day 16. (B) Individual tumor volumes, where each line represents a single mouse. P-values were calculated on Day 12. (C) Kaplan-Meier survival curve and proportion of tumor clearance in each treatment group. (D-E) Mice in complete remission for more than 3 months following last monotherapy or combination treatment and naïve BALB/c mice were challenged with (D) 0.25 x 10^6 EMT-6 cells or (E) 0.5 x 10^5 4T1 cells by orthotopic injection on the opposite mammary pad of the original tumor site. Average tumor volume after implantation. Error bars represent SEM. N/A = not available.

NHS-muIL12 contributed mainly to NK cell activation, maturation, and cytotoxicity in both the spleen and TME.

Although BA monotherapy slightly decreased T_{regs} in the MC38 model, NHS-muIL12 and BA combination therapy further decreased T_{regs} relative to BA monotherapy, but not NHS-muIL12 monotherapy, suggesting that NHS-muIL12 plays a greater role in modulating T_{regs} in the combination therapy. This enhanced reduction of T_{regs} with NHS-muIL12 could be due to IL-12 inhibition of TGF-β-induced T_{reg} development [43]. Independent of BA, NHS-muIL12 may be abrogating TGF-β-driven development of T_{regs} in the TME. Despite each component of the combination therapy eliciting different immune effects, NHS-IL12 and BA combination therapy significantly increased the ratio of CD8$^+$ TILs to infiltrating T_{regs} relative to either monotherapy, suggesting that the molecules have complementary and additive effects when combined.

T-bet stimulates the expression of IFN-γ, FasL, and Prf1, regulates cytotoxicity of CD8$^+$ T cells, and sustains memory T cell subsets [44–46]. NHS-muIL12 and BA combination therapy significantly increased splenic T-bet$^+$ CD8$^+$T cells relative to NHS-muIL12 and BA monotherapies, suggesting potential additive effects on this cell population. The fact that NHS-muIL12 and BA combination therapy significantly increased CD8$^+$ T cells expressing CXCR3 relative to either monotherapy further suggests a potentially important role for CTLs in the mechanism of action of NHS-muIL12 and BA combination therapy. Indeed, results from a recent publication suggest that CXCR3-mediated trafficking of CD8$^+$ T cells to the tumor is necessary for an effective

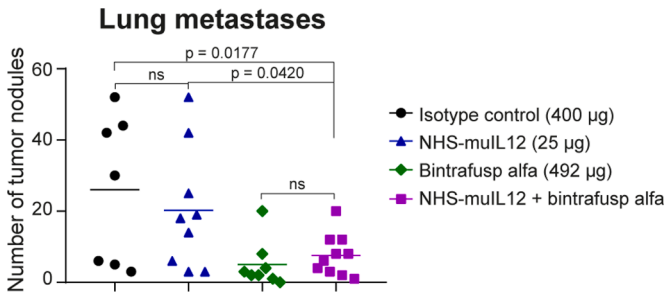

Fig. 5. Combination therapy with NHS-muIL12 and BA reduced spontaneous lung metastases in 4T1 tumor-bearing mice, similar to BA monotherapy. Jh mice bearing 4T1 orthotopic tumors (30–50 mm^3) ($n = 7$–10 mice/group) were treated with: isotype control (400 µg iv; Day 0, 4, 7, 11, 14), NHS-muIL12 (25 µg sc; Day 0), BA (492 µg iv Day 0, 4, 7, 11, 14), or NHS-muIL12 + BA. Lung metastases were quantified at Day 25 or when mice were sacrified because their tumors reached 1000 mm^3; mice that were sacrificed prior to Day 25 due to health concerns were not included in the analysis.

antitumor immune response to anti–PD-1 therapy [47].

Currently, cancer immunotherapy research mainly focuses on antitumor activity of CTLs as a major driver of adaptive immunity. However, $CD4^+$ T cells also play an important role in the antitumor activity. Although $CD4^+$ T cells can differentiate into multiple subtypes that may play opposing roles in antitumor immunity [48,49], IL-12 induces the differentiation of naïve Th cells towards a Th1 phenotype and the production of cytokines such as IFN-γ and tumor associated factor alpha (TNF-α) to promote cell-mediated immunity [48,49]. The Th1 subset of $CD4^+$ T cells are key to adaptive immunity, and priming of CTL responses depends on innate signals relayed from $CD4^+$ T cells to $CD8^+$ T cells [50,51]. On the other hand, NHS-muIL12 and BA treatment can significantly decrease the subpopulation of $CD4^+$ T_{regs}, which plays an important role in cancer immune suppression. NHS-muIL12 and BA may synergize to increase these $CD4^+$ Th1 cell populations to assist the priming of tumor-specific CTLs and decrease T_{regs} to diminish immune suppression, thereby contributing to enhanced antitumor activity with the combination therapy.

NHS-muIL12 and BA combination therapy further enhanced activation of NK cells relative to either monotherapy, suggesting possible synergy between the two molecules in the activation of an innate immune response. This is supported by previous studies that suggested NHS-muIL12 may act as a bridge to link innate and adaptive immunity [24] and data that BA can increase the density of NK cells expressing activating receptors and an NK growth factor receptor [33].

Results showing that NHS-muIL12 and BA combination therapy increased $CD8^+$ T_{EM} relative to NHS-muIL12 monotherapy are consistent with previous findings that BA induces $CD8^+$ T_{EM} cells in the TME of MC38 and EMT-6 models [33] and are consistent with BA monotherapy and NHS-muIL12 and BA combination therapy being resistant to tumor rechallenge in these models. ELISpot also demonstrated that combination therapy of BA and NHS-muIL12 further increased the frequency of tumor antigen specific immune memory $CD8^+$ T cells relative to either monotherapy.

BA monotherapy has recently been shown to significantly reduce EMT and mesenchymal markers in human non-small cell lung cancer xenografts [52]. BA can also reduce collagen deposition and cancer associated fibroblasts (CAFs) [33], which play a role in metastasis, and can decrease spontaneous metastases in mouse models [33]. In the current study, we found that decreased metastases with BA and NHS-muIL12 combination therapy in the 4T1 model was driven mainly by BA. These results are consistent with the link between PD-L1 and the EMT [53,54] and the known role of TGF-β-induced EMT in driving tumor invasion and metastasis [55].

Collectively, these preclinical findings strengthen the rationale for the combination of NHS-IL12 and BA and highlight the potential clinical development of this combination for the treatment of patients with solid tumors.

CRediT authorship contribution statement

Chunxiao Xu: Conceptualization, Methodology, Validation, Formal analysis, Investigation, Data curation, Writing – review & editing, Visualization, Supervision. **Bo Marelli:** Investigation, Methodology, Validation, Formal analysis. **Jin Qi:** Investigation, Methodology, Validation, Formal analysis. **Guozhong Qin:** Investigation, Methodology, Validation, Formal analysis. **Huakui Yu:** Investigation, Methodology, Validation, Formal analysis. **Hong Wang:** Investigation, Methodology, Validation, Formal analysis. **Molly H. Jenkins:** Writing – original draft, Writing – review & editing, Formal analysis, Visualization. **Kin-Ming Lo:** Conceptualization, Supervision, Project administration. **Yan Lan:** Conceptualization, Supervision, Project administration.

Declaration of Competing Interest

The authors are all employees of EMD Serono Research & Development Institute, Inc., Billerica, MA, USA, an affiliate of Merck KGaA, Darmstadt, Germany. Kin-Ming Lo is the inventor on the US Patent 9676,863 B2, “Targeted TGF-β inhibition”, issued June 13, 2017, and held by the Merck Patent GmbH, covering M7824 (bintrafusp alfa), its methods of making, and its methods of use. All other authors disclose no competing interests.

Financial support

This study was sponsored by Merck KGaA, Darmstadt, Germany.

Acknowledgments

The authors thank Melissa Derner for assistance with reviewing and editing the manuscript. This study was funded and supported by EMD Serono Research and Development Institute, Inc, Billerica, MA, USA, an affiliate of Merck KGaA, Darmstadt, Germany.

Supplementary materials

Supplementary material associated with this article can be found, in the online version, at doi:10.1016/j.tranon.2021.101322.

References

[1] P. Sharma, S. Hu-Lieskovan, J.A. Wargo, R.A. Primary, Adaptive, and acquired resistance to cancer immunotherapy, Cell 168 (4) (2017) 707–723, https://doi.org/10.1016/j.cell.2017.01.017. PubMed PMID: 28187290.

[2] P.S. Hegde, V. Karanikas, S. Evers, The Where, the when, and the how of immune monitoring for cancer immunotherapies in the era of checkpoint inhibition, Clin. Cancer Res. 22 (8) (2016) 1865–1874, https://doi.org/10.1158/1078-0432.ccr-15-1507. Epub 2016/04/17PubMed PMID: 27084740.

[3] J. Galon, A. Costes, F. Sanchez-Cabo, A. Kirilovsky, B. Mlecnik, C. Lagorce-Pages, et al., Type, density, and location of immune cells within human colorectal tumors predict clinical outcome, Science 313 (5795) (2006) 1960–1964, https://doi.org/10.1126/science.1129139. Epub 2006/09/30PubMed PMID: 17008531.

[4] J. Galon, D. Bruni, Approaches to treat immune hot, altered and cold tumours with combination immunotherapies, Nat. Rev. Drug Discov. 18 (3) (2019) 197–218, https://doi.org/10.1038/s41573-018-0007-y.

[5] B. Mlecnik, G. Bindea, A. Kirilovsky, H.K. Angell, A.C. Obenauf, M. Tosolini, et al., The tumor microenvironment and Immunoscore are critical determinants of dissemination to distant metastasis, Sci. Transl. Med. 8 (327) (2016), https://doi.org/10.1126/scitranslmed.aad6352, 327ra26. Epub 2016/02/26PubMed PMID: 26912905.

[6] A. Calon, E. Lonardo, A. Berenguer-Llergo, E. Espinet, X. Hernando-Momblona, M. Iglesias, et al., Stromal gene expression defines poor-prognosis subtypes in colorectal cancer, Nat. Genet. 47 (4) (2015) 320–329, https://doi.org/10.1038/ng.3225. Epub 2015/02/24PubMed PMID: 25706628.

[7] L. Peng, X.Q. Yuan, C.Y. Zhang, F. Ye, H.F. Zhou, W.L. Li, et al., High TGF-β1 expression predicts poor disease prognosis in hepatocellular carcinoma patients, Oncotarget 8 (21) (2017) 34387–34397, https://doi.org/10.18632/oncotarget.16166. PubMed PMID: 28415739.

[8] H.T. Marshall, M.B.A. Djamgoz, Immuno-oncology: emerging targets and combination therapies, Front. Oncol. 8 (2018) 315, https://doi.org/10.3389/fonc.2018.00315. PubMed PMID: 30191140.

[9] J. Kim, C. Heery, M. Bilusic, N. Singh, R. Madan, H. Sabzevari, et al., First-in-human phase I trial of NHS-IL12 in advanced solid tumors, ASCO Annu. Meet. Proc. 30 (15) (2012) TPS2617.

[10] M.W. Teng, E.P. Bowman, J.J. McElwee, M.J. Smyth, J.L. Casanova, A.M. Cooper, et al., IL-12 and IL-23 cytokines: from discovery to targeted therapies for immune-mediated inflammatory diseases, Nat. Med. 21 (7) (2015) 719–729, https://doi.org/10.1038/nm.3895. Epub 2015/06/30PubMed PMID: 26121196.

[11] V. Athie-Morales, H.H. Smits, D.A. Cantrell, C.M. Hilkens, Sustained IL-12 signaling is required for Th1 development, J. Immunol. 172 (1) (2004) 61–69. Epub 2003/12/23PubMed PMID: 14688310.

[12] G. Trinchieri, Interleukin-12 and the regulation of innate resistance and adaptive immunity, Nat. Rev. Immunol. 3 (2) (2003) 133–146, https://doi.org/10.1038/nri1001.

[13] E.D. Tait Wojno, C.A. Hunter, J.S Stumhofer, The Immunobiology of the interleukin-12 family: room for discovery, Immunity 50 (4) (2019) 851–870, https://doi.org/10.1016/j.immuni.2019.03.011. Epub 2019/04/18PubMed PMID: 30995503; PubMed Central PMCID: PMCPMC6472917.

[14] M. Del Vecchio, E. Bajetta, S. Canova, M.T. Lotze, A. Wesa, G. Parmiani, et al., Interleukin-12: biological properties and clinical application, Clin. Cancer Res. 13 (16) (2007) 4677–4685, https://doi.org/10.1158/1078-0432.ccr-07-0776. Epub 2007/08/19PubMed PMID: 17699845.

[15] U. Grohmann, M.L. Belladonna, R. Bianchi, C. Orabona, E. Ayroldi, M.C. Fioretti, et al., IL-12 acts directly on DC to promote nuclear localization of NF-kappaB and primes DC for IL-12 production, Immunity 9 (3) (1998) 315–323. PubMed PMID: 9768751.

[16] M. Eisenring, J. vom Berg, G. Kristiansen, E. Saller, B. Becher, IL-12 initiates tumor rejection via lymphoid tissue-inducer cells bearing the natural cytotoxicity receptor NKp46, Nat. Immunol. 11 (11) (2010) 1030–1038, https://doi.org/10.1038/ni.1947. Epub 2010/10/12PubMed PMID: 20935648.

[17] J.A. Gollob, E.A. Murphy, S. Mahajan, C.P. Schnipper, J. Ritz, D.A. Frank, Altered interleukin-12 responsiveness in Th1 and Th2 cells is associated with the differential activation of STAT5 and STAT1, Blood 91 (4) (1998) 1341–1354, https://doi.org/10.1182/blood.V91.4.1341.

[18] R.D. Alvarez, M.W. Sill, S.A. Davidson, C.Y. Muller, D.P. Bender, R.L. DeBernardo, et al., A phase II trial of intraperitoneal EGEN-001, an IL-12 plasmid formulated with PEG-PEI-cholesterol lipopolymer in the treatment of persistent or recurrent epithelial ovarian, fallopian tube or primary peritoneal cancer: a gynecologic oncology group study, Gynecol. Oncol. 133 (3) (2014) 433–438, https://doi.org/10.1016/j.ygyno.2014.03.571. Epub 2014/04/09PubMed PMID: 24708919; PubMed Central PMCID: PMCPMC4057915.

[19] K. Anwer, F.J. Kelly, C. Chu, J.G. Fewell, D. Lewis, R.D. Alvarez, Phase I trial of a formulated IL-12 plasmid in combination with carboplatin and docetaxel chemotherapy in the treatment of platinum-sensitive recurrent ovarian cancer, Gynecol. Oncol. 131 (1) (2013) 169–173, https://doi.org/10.1016/j.ygyno.2013.07.081. Epub 2013/07/19PubMed PMID: 23863356.

[20] I. Etxeberria, E. Bolanos, J.I. Quetglas, A. Gros, A. Villanueva, J. Palomero, et al., Intratumor Adoptive Transfer of IL-12 mRNA Transiently Engineered Antitumor CD8(+) T Cells, Cancer Cell 36 (6) (2019) 613–629, https://doi.org/10.1016/j.ccell.2019.10.006, e7. Epub 2019/11/26PubMed PMID: 31761658.

[21] E.L. McMichael, B. Benner, L.S. Atwal, N.B. Courtney, X. Mo, M.E. Davis, et al., A phase I/II trial of cetuximab in combination with interleukin-12 administered to patients with unresectable primary or recurrent head and neck squamous cell carcinoma, Clin. Cancer Res. 25 (16) (2019) 4955–4965, https://doi.org/10.1158/1078-0432.ccr-18-2108. Epub 2019/05/31PubMed PMID: 31142501; PubMed Central PMCID: PMCPMC6697573.

[22] J. Fallon, R. Tighe, G. Kradjian, W. Guzman, A. Bernhardt, B. Neuteboom, et al., The immunocytokine NHS-IL12 as a potential cancer therapeutic, Oncotarget 5 (7) (2014) 1869–1884, https://doi.org/10.18632/oncotarget.1853. PubMed PMID: 24681847; PubMed Central PMCID: PMC4039112.

[23] J. Strauss, C.R. Heery, J.W. Kim, C. Jochems, R.N. Donahue, A.S. Montgomery, et al., First-in-human phase I trial of a tumor-targeted cytokine (NHS-IL12) in subjects with metastatic solid tumors, Clin. Cancer Res. 25 (1) (2019) 99–109, https://doi.org/10.1158/1078-0432.ccr-18-1512.

[24] C. Xu, Y. Zhang, P.A. Rolfe, V.M. Hernandez, W. Guzman, G. Kradjian, et al., Combination therapy with NHS-muIL12 and avelumab (anti-PD-L1) enhances antitumor efficacy in preclinical cancer models, Clin. Cancer Res. 23 (19) (2017) 5869–5880, https://doi.org/10.1158/1078-0432.ccr-17-0483, an official journal of the American Association for Cancer ResearchEpub 2017/07/07PubMed PMID: 28679778.

[25] J. Strauss, Y. Vugmeyster, M. Sznol, R.K. Pachynski, K. Trang, S. Chennoufi, et al., 1224PPhase Ib, open-label, dose-escalation study of M9241 (NHS-IL12) plus avelumab in patients (pts) with advanced solid tumours, Ann. Oncol. 30 (Supplement_5) (2019), https://doi.org/10.1093/annonc/mdz253.050.

[26] J.M. Yingling, K.L. Blanchard, J.S. Sawyer, Development of TGF-beta signalling inhibitors for cancer therapy, Nat. Rev. Drug Discov. 3 (12) (2004) 1011–1022, https://doi.org/10.1038/nrd1580. Epub 2004/12/02PubMed PMID: 15573100.

[27] J.C. Neel, L. Humbert, J.J Lebrun, The dual role of TGFβ in human cancer: from tumor suppression to cancer metastasis, ISRN Mol. Biol. (2012), https://doi.org/10.5402/2012/381428, 2012:28.

[28] C. Neuzillet, A. Tijeras-Raballand, R. Cohen, J. Cros, S. Faivre, E. Raymond, et al., Targeting the TGFbeta pathway for cancer therapy, Pharmacol. Ther. 147 (2015) 22–31, https://doi.org/10.1016/j.pharmthera.2014.11.001. Epub 2014/12/03PubMed PMID: 25444759.

[29] H. Xu, G.X. Zhang, M. Wysocka, C.Y. Wu, G. Trinchieri, A. Rostami, The suppressive effect of TGF-beta on IL-12-mediated immune modulation specific to a peptide Ac1-11 of myelin basic protein (MBP): a mechanism involved in inhibition of both IL-12 receptor beta1 and beta2, J. Neuroimmunol. 108 (1–2) (2000) 53–63. Epub 2000/07/20PubMed PMID: 10900337.

[30] C.S. Hirsch, R. Hussain, Z. Toossi, G. Dawood, F. Shahid, J.J. Ellner, Cross-modulation by transforming growth factor beta in human tuberculosis: suppression of antigen-driven blastogenesis and interferon gamma production, Proc. Natl. Acad. Sci. USA 93 (8) (1996) 3193–3198, https://doi.org/10.1073/pnas.93.8.3193. PubMed PMID: 8622912.

[31] C. Pardoux, X. Ma, S. Gobert, S. Pellegrini, P. Mayeux, F. Gay, et al., Downregulation of interleukin-12 (IL-12) responsiveness in human T cells by transforming growth factor-beta: relationship with IL-12 signaling, Blood 93 (5) (1999) 1448–1455. Epub 1999/02/25PubMed PMID: 10029570.

[32] J.J. Bright, S. Sriram, TGF-beta inhibits IL-12-induced activation of Jak-STAT pathway in T lymphocytes, J Immunol 161 (4) (1998) 1772–1777. Epub 1998/08/26PubMed PMID: 9712043.

[33] Y. Lan, D. Zhang, C. Xu, K.W. Hance, B. Marelli, J. Qi, et al., Enhanced preclinical antitumor activity of M7824, a bifunctional fusion protein simultaneously targeting PD-L1 and TGF-beta, Sci. Transl. Med. 10 (424) (2018), https://doi.org/10.1126/scitranslmed.aan5488. PubMed PMID: 29343622.

[34] Y. Lan, M. Moustafa, M. Knoll, C. Xu, J. Furkel, A. Lazorchak, et al., Simultaneous targeting of TGF-beta/PD-L1 synergizes with radiotherapy by reprogramming the tumor microenvironment to overcome immune evasion, Cancer Cell (2021), https://doi.org/10.1016/j.ccell.2021.08.008. PubMed PMID: 34506739.

[35] J. Strauss, C.R. Heery, J. Schlom, R.A. Madan, L. Cao, Z. Kang, et al., Phase I trial of M7824 (MSB0011359C), a bifunctional fusion protein targeting PD-L1 and TGFβ, in advanced solid tumors, Clin.Cancer Res. 24 (6) (2018) 1287–1295, https://doi.org/10.1158/1078-0432.ccr-17-2653.

[36] M. Khasraw, M. Weller, D. Lorente, K. Kolibaba, C.K. Lee, C. Gedye, et al., Bintrafusp alfa (M7824), a bifunctional fusion protein targeting TGF-beta and PD-L1: results from a phase I expansion cohort in patients with recurrent glioblastoma, Neurooncol. Adv. 3 (1) (2021) vdab058, https://doi.org/10.1093/noajnl/vdab058. PubMed PMID: 34056607; PubMed Central PMCID: PMCPMC8156979.

[37] C.C. Lin, T. Doi, K. Muro, M.M. Hou, T. Esaki, H. Hara, et al., Bintrafusp alfa, a bifunctional fusion protein targeting TGFbeta and PD-L1, in patients with esophageal squamous cell carcinoma: results from a phase 1 cohort in Asia, Target Oncol. 16 (4) (2021) 447–459, https://doi.org/10.1007/s11523-021-00810-9. PubMed PMID: 33840050; PubMed Central PMCID: PMCPMC8266718.

[38] B.C. Cho, A. Daste, A. Ravaud, S. Salas, N. Isambert, E. McClay, et al., Bintrafusp alfa, a bifunctional fusion protein targeting TGF-beta and PD-L1, in advanced squamous cell carcinoma of the head and neck: results from a phase I cohort, J Immunother. Cancer 8 (2) (2020), https://doi.org/10.1136/jitc-2020-000664. PubMed PMID: 32641320; PubMed Central PMCID: PMCPMC7342865.

[39] J. Strauss, M.E. Gatti-Mays, B.C. Cho, A. Hill, S. Salas, E. McClay, et al., Bintrafusp alfa, a bifunctional fusion protein targeting TGF-beta and PD-L1, in patients with human papillomavirus-associated malignancies, J. Immunother. Cancer 8 (2) (2020), https://doi.org/10.1136/jitc-2020-001395. PubMed PMID: 33323462; PubMed Central PMCID: PMCPMC7745517.

[40] L. Paz-Ares, T.M. Kim, D. Vicente, E. Felip, D.H. Lee, K.H. Lee, et al., Bintrafusp alfa, a bifunctional fusion protein targeting TGF-beta and PD-L1, in second-line treatment of patients with NSCLC: results from an expansion cohort of a phase 1 trial, J. Thorac. Oncol. 15 (7) (2020) 1210–1222, https://doi.org/10.1016/j.jtho.2020.03.003. PubMed PMID: 32173464; PubMed Central PMCID: PMCPMC8210474.

[41] S.A. Niglio, Girardi DdM, L.M. Cordes, L. Ley, M. Mallek, O.S. Ortiz, et al., A phase I study of bintrafusp alfa (M7824) and NHS-IL12 (M9241) alone and in combination with stereotactic body radiation therapy (SBRT) in adults with metastatic non-prostate genitourinary malignancies, J. Clin. Oncol. 39 (15_suppl) (2021), https://doi.org/10.1200/JCO.2021.39.15_suppl.TPS4599. TPS4599-TPS.

[42] M.O. Atiq, M. Bilusic, F. Karzai, L.M. Cordes, J. Strauss, H.A. Sater, et al., A phase I/II study of bintrafusp alfa and NHS-IL12 in combination with docetaxel in adults with metastatic castration sensitive (mCSPC) and castration-resistant prostate cancer (mCRPC), J. Clin. Oncol. 39 (15_suppl) (2021), https://doi.org/10.1200/JCO.2021.39.15_suppl.TPS5096. TPS5096-TPS.

[43] J. Prochazkova, K. Pokorna, V. Holan, IL-12 inhibits the TGF-beta-dependent T cell developmental programs and skews the TGF-beta-induced differentiation into a Th1-like direction, Immunobiology 217 (1) (2012) 74–82, https://doi.org/10.1016/j.imbio.2011.07.032. Epub 2011/09/10PubMed PMID: 21903294.

[44] J.J. Knox, G.L. Cosma, M.R. Betts, L.M. McLane, Characterization of T-bet and eomes in peripheral human immune cells, Front. Immunol. 5 (2014) 217, https://doi.org/10.3389/fimmu.2014.00217. Epub 2014/05/27PubMed PMID: 24860576; PubMed Central PMCID: PMCPMC4030168.

[45] V. Lazarevic, L.H. Glimcher, G.M. Lord, T-bet: a bridge between innate and adaptive immunity, Nat. Rev. Immunol. 13 (11) (2013) 777–789, https://doi.org/10.1038/nri3536. Epub 2013/10/12PubMed PMID: 24113868.

[46] K. Eshima, K. Misawa, C. Ohashi, K. Iwabuchi, Role of T-bet, the master regulator of Th1 cells, in the cytotoxicity of murine CD4(+) T cells, Microbiol. Immunol. 62 (5) (2018) 348–356, https://doi.org/10.1111/1348-0421.12586. Epub 2018/03/27PubMed PMID: 29577371.

[47] Z.S. Chheda, R.K. Sharma, V.R. Jala, A.D. Luster, B. Haribabu, Chemoattractant receptors BLT1 and CXCR3 regulate antitumor immunity by facilitating CD8+ T Cell migration into tumors, J. Immunol. 197 (5) (2016) 2016–2026, https://doi.org/10.4049/jimmunol.1502376. Epub 07/27PubMed PMID: 27465528.

[48] T. Ahrends, J. Borst, The opposing roles of CD4(+) T cells in anti-tumour immunity, Immunology (2018), https://doi.org/10.1111/imm.12941. PubMed PMID: 29700809; PubMed Central PMCID: PMCPMC6050207.
[49] H.J. Kim, H. Cantor, CD4 T-cell subsets and tumor immunity: the helpful and the not-so-helpful, Cancer Immunol. Res. 2 (2) (2014) 91–98, https://doi.org/10.1158/2326-6066.CIR-13-0216. PubMed PMID: 24778273.
[50] J. Borst, T. Ahrends, N. Babala, C.J.M. Melief, W. Kastenmuller, CD4(+) T cell help in cancer immunology and immunotherapy, Nat. Rev. Immunol. 18 (10) (2018) 635–647, https://doi.org/10.1038/s41577-018-0044-0. PubMed PMID: 30057419.
[51] S. Bedoui, W.R. Heath, S.N. Mueller, CD4(+) T-cell help amplifies innate signals for primary CD8(+) T-cell immunity, Immunol. Rev. 272 (1) (2016) 52–64, https://doi.org/10.1111/imr.12426. Epub 2016/06/21PubMed PMID: 27319342.
[52] J.M. David, C. Dominguez, K.K. McCampbell, J.L. Gulley, J. Schlom, C. Palena, A novel bifunctional anti-PD-L1/TGF-beta Trap fusion protein (M7824) efficiently reverts mesenchymalization of human lung cancer cells, Oncoimmunology 6 (10) (2017), e1349589, https://doi.org/10.1080/2162402x.2017.1349589. Epub 2017/11/11PubMed PMID: 29123964; PubMed Central PMCID: PMCPMC5665067.
[53] S. Tsutsumi, H. Saeki, Y. Nakashima, S. Ito, E. Oki, M. Morita, et al., Programmed death-ligand 1 expression at tumor invasive front is associated with epithelial-mesenchymal transition and poor prognosis in esophageal squamous cell carcinoma, Cancer Sci. 108 (6) (2017) 1119–1127, https://doi.org/10.1111/cas.13237. Epub 2017/03/16PubMed PMID: 28294486; PubMed Central PMCID: PMCPMC5480087.
[54] C.Y. Ock, S. Kim, B. Keam, M. Kim, T.M. Kim, J.H. Kim, et al., PD-L1 expression is associated with epithelial-mesenchymal transition in head and neck squamous cell carcinoma, Oncotarget 7 (13) (2016) 15901–15914, https://doi.org/10.18632/oncotarget.7431. Epub 2016/02/20PubMed PMID: 26893364; PubMed Central PMCID: PMCPMC4941285.
[55] R.J. Akhurst, A. Hata, Targeting the TGFbeta signalling pathway in disease, Nat. Rev. Drug Discov. 11 (10) (2012) 790–811, https://doi.org/10.1038/nrd3810. Epub 2012/09/25PubMed PMID: 23000686; PubMed Central PMCID: PMCPMC3520610.